Verification of results of the working technology SNOWE for snow water equivalent and snow density fields determination as initial data for COSMO model

E. Kazakova, I. Rozinkina, M. Chumakov

1 Introduction

Atmospheric models need snow water equivalent (SWE) and snow density values as initial fields. However, currently no operational SWE measurements are carried out with the spatial and temporal resolution needed for mesoscale models. Only seasonal specific observations are conducted in 5-10 days interval SYNOP measurements of snow depth is the only regular operational information describing snow cover characteristics, since satellite data contain information only on the position of snow cover boundary. Snow density calculation is based on 'age functions', which describes snow evolution quite robust. SWE is obtained from these snow density values and measurements of snow depth. The snow density values depend on thermal history of the entire cold period of the year.

These values could be obtained using empirical relationships, which allow converting snow depth into needed density values, which results of SWE simulation during continuous data assimilation system (DAS) cycles resulting in turn in accumulation of errors. According to the previous research [Kazakova, Rozinkina, 2011], COSMO-Ru model simulates SWE with discrepancies (relative errors of the model versus measured SWE values could be as high as $200 - 300\%$. RMS errors were about 10 mm at the southern European part of Russia and up to 130 mm in the North) independently of snow parameterization used in the model. This results in wrong calculation of heat budget components near snow edge and wrong T2m forecasts in this narrow frontier zone.

2 Goals

For NWP purposes there is a need to use only station observations as the most reliable source of information on snow cover. Therefore it is required to develop such an algorithm which could allow to calculate snow cover characteristics using only the data of standard meteorological observations (in SYNOP code) transmitted every 3 hours. Such algorithm should consider the main processes in snow cover during its existing period, which could be described only using station observations without excessive details, which could significantly increase the computational time of snow characteristics assessment. A snow model satisfying these requirements is presented in further sections. Based on this snow model, the technology of SWE and snow density initial fields generation was developed. The results of its processing in quasi-operational regime in winter 2014/2015 are discussed.

3 Brief description of the snow model SMFE

Developed one-dimensional multi-layer parametric snow model SMFE (Snow Model Finite Element) is based on standard meteorological observations – snow depth, air temperature, dew point temperature, wind speed, 12-hour accumulated precipitation [Kazakova, Chumakov, Rozinkina, 2013].The realized SMFE model is based on the main principle that snow column is represented as a number of layers (hereinafter referred as elements) which are in thermal and mechanical interaction with each other. The height of an element h in the given realization is set to 1 cm in accordance with the accuracy of this characteristic within the framework of SYNOP-code. Consequently, the number of elements is counted according the measured snow depth (cm) at each station. Since in time $t_0, t_1, \ldots, t_k$ (during 'snow' season) snow depth at station changes, the number of elements will also change.Brief description of the algorithm principle is presented on the scheme (Fig.1).

The model starts operating as soon as the measured snow depth differs from zero. At each time step (1 day) the amount of new elements in dependence on snow depth variations $\triangle H$ is defined: $N_{t_k} = N_{(t_{k-1})} + \triangle N$ where $\triangle N = \triangle H/h$.

If $\triangle N > 0$ (case of snow falling, then density of the newly fallen upper layers (fresh snow with depth $\triangle H$),is calculated in dependence on daily-averaged air temperature according to empirical equation 1 [Bartlett, MacKay, Verseghy, 2006]:

$\rho_{s,f} = 67.92 + 52.25^{\frac{T_a}{2.59}}, T_a \leqslant 0^oC$; $\rho_{s,f} = min(200; 119.2 + 20T_a), T_a > 0^oC$;

where $\rho_{s,f}$ - fresh snow density,kg/m^3,

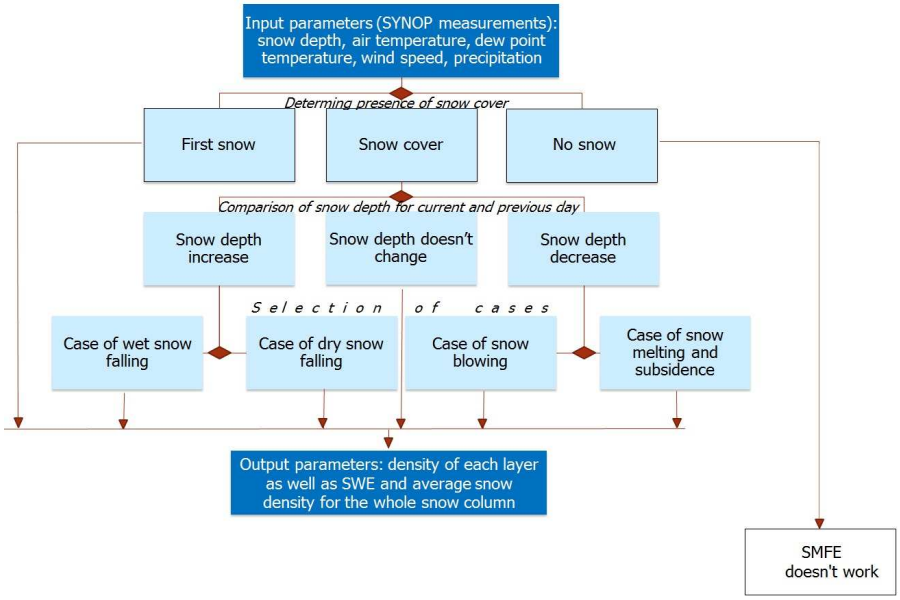

Figure 1: The schematic diagramme of the model SMFE. Dark blue rectangles represent the input and output parameters.

For 'lying' snow (not considering new 'fresh snow' layers) variation of element density at each time step $\triangle\rho_n(t_k) = \rho_n(t_{k-1}) + \triangle\rho$, (where $n(t_k) = 1, \ldots, N(t_k)$ is a serial number of an element),is determined, when $\triangle N \neq 0$. Component $\triangle\rho$ contains information about increase/decrease of an element density in dependence on the value of $\triangle N$:

$\triangle\rho = \rho + \rho + \rho$

where ρ - case of snow compaction on account of new elements($\triangle N > 0$), ρ - case of snow compaction due to snow blowing ($\triangle N < 0$), ρ - case of snow compaction dew to subsidence or melting (percolation of water and its freezing)($\triangle N < 0$). If $\triangle N > 0$, the density of each element

$$\rho_n(t_k = \rho_n(t_k))T_n(t_{k\smile}), \sum_{m=n(t_k)}^{N(t_k)} \rho_m(t_k) \tag{1}$$

would be a function, depending on air temperature $T_n(t_{k\smile})$ at time $(t_{k\smile})$, when snow was fallen, and the amount of layers which affect it from above. It is assumed that in the moment of holding of snow depth measurement all the layers inside the column are in quasi-static equilibrium, i.e. experiencing only elastic deformation under gravity.

For determination of density of these layers formulae based on [Yosida, Huzioka, 1954] with consideration of empirical parameter responsible for changing of element's size under permanent deformation related to pressure of overlying elements [Epifanov, Osokin, 2010]) were used:

$$\rho = \frac{\frac{mg}{10^6(1-\sigma)} + 1.86}{0.0167}, T > -5^oC; \rho = \frac{\frac{mg}{10^6(1-\sigma)} + 10.8}{0.059}, T \leq -5^oC \tag{2}$$

where $m = H \cdot (\rho_1 + \rho_2 + \ldots), H = 0.01m$, $\rho_1.\rho_2, \ldots$ - densities of the first, second, etc. elements.

Obviously, during the process of snow accumulation, layers ('inclusions') will be distinguished in snow column, which have quite homogeneous density being determined in dependence on temperature (i.e. large layers formed at different temperature conditions of snow falling could be found).

If snow depth is stable for one day and further, the number of elements didn't change ($\triangle N = 0$). Provided no precipitation, snow density and SWE don't have variations; otherwise equal amount of moisture is added to each element.

In SMFE it is suggested that snow depth decrease ($\triangle N < 0$) is calculated on the basis of analysis of measured values of meteorological parameters: melting took place when there are positive temperatures during a day,

snow blowing – when there are negative temperatures in case of significant snow depth decrease; in other cases it is suggested that snow subsidence took place.

In case of snow subsidence mass redistribution between elements in all 'inclusions' is performed by sequential exclusion of layers with minimum density with their mass redistribution to all the layers until the measured snow depth value at a certain time will be achieved.

Mass of melted snow is defined regarding the decrease of the depth of snow cover with earlier determined density. Clear that a part of formed water is removed due to runoff and a part is redistributed is snow thickness. Following this assumption recalculation of density of each layer is made. In case of snow blowing a part of snow is also removed (although it breaks the general picture of the mass balance, however, 'move' the picture of simulated snow in accordance with the measurement data). Each time step in SMFE calculation of evaporation from snow is possible, according to [Kuzmin, 1961].

It is suggested that maximum snow density in the model doesn't exceed density of porous ice equal to about 700 kg/m^3.

Every day snow water equivalent $SWE_{(tk)}$ is calculated as a sum of densities ρ_n of all the layers and snow column density, $\rho_{(tk)}$ – as an averaged value of all the layers:

$$SWE(t_k) = \sum_{n=1}^{N(t_k)} \rho_{n(tk)}(t_k) \cdot h, \rho_{(tk)} = \frac{1}{N_{(tk)}} \sum_{n=1}^{N(t_k)} \rho_{n(t_k)}(t_k) \quad (3)$$

Computational algorithm of the model is realized in Fortran-90.

Reliable testing results of SMFE model were presented in [Kazakova, Chumakov, Rozinkina, 2013], which show good compliance with observations. Example of comparison of SWE measurements, SWE field based on SMFE and COSMO initial SWE field are shown in Fig.4.

4 SWE technology and snow density analysis (SNOWE technology)

On the basis of developed snow model was developed a technology for preparation of initial fields of SWE and snow density (SNOWE technology). The general scheme is presented on Fig.2. During the 'snow' season 2014/2015 the proposed technology was tested in quasi-operational mode at Hydrometcenter of Russia. Forecasts were produced starting from 00 UTC every day for two domains of COSMO-Ru model - for the territories of Central and East Europe and European part of Russia (COSMO-Ru7 - grid step 7 km) and for territory of Central Russia (COSMO-Ru2, grid step 2.2 km) (Fig.3).

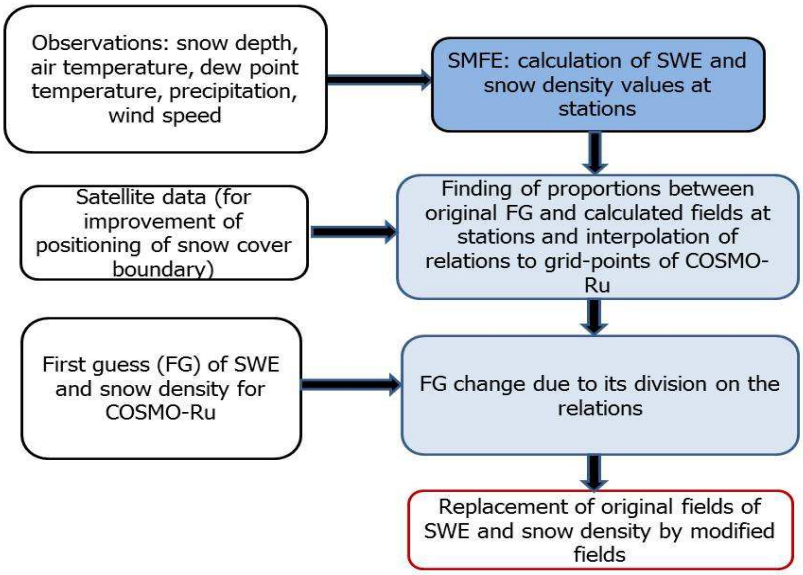

Figure 2: Technological scheme for preparation of initial fields of SWE and snow density at Hydrometcenter of Russia.

The SMFE model generates SWE and snow density values for stations based on daily SYNOP measurements.

Observations from 2296 stations were used for COSMO-Ru7 area, the quality control of snow depth and T2m measurements was performed.

As a first step for Objective Analysis (OA), the FG data (gridded values of SWE and snow density from initial data (based on the global DAS) for COSMO-Ru) is interpolated from COSMO-Ru grid points to the points of SMFE calculations (points of observations). For these points the proportions between COSMO-values and SMFE-values are determined. Than these relations are interpolated to the grid points of COSMO-Ru to correct the initial fields. The interpolation of obtained local values of proportions to the grid-points of COSMO model was realized on the basis of Delaunay triangulation. At this step satellite data with 4-km resolution from NOAA server (ftp://140.90.213.161/autosnow/4kmNH/) was used for improvement of positioning of snow cover boundary. Finally, the normalized FG of SWE and snow density are used as initial fields.

Tests demonstrated small differences between the results of direct interpolation of SWE values from SMFE to COSMO-grid and proposed OA technology in case of dense observational network (COSMO-Ru2).

The zone with maximum changes of meteorological elements during the 'snow period' is the zone close to the snow boundary, especially during snow melting. Changes in air temperature especially and other meteorological parameters will be viewed with changes of initial fields of SWE and snow density in this boundary zone.

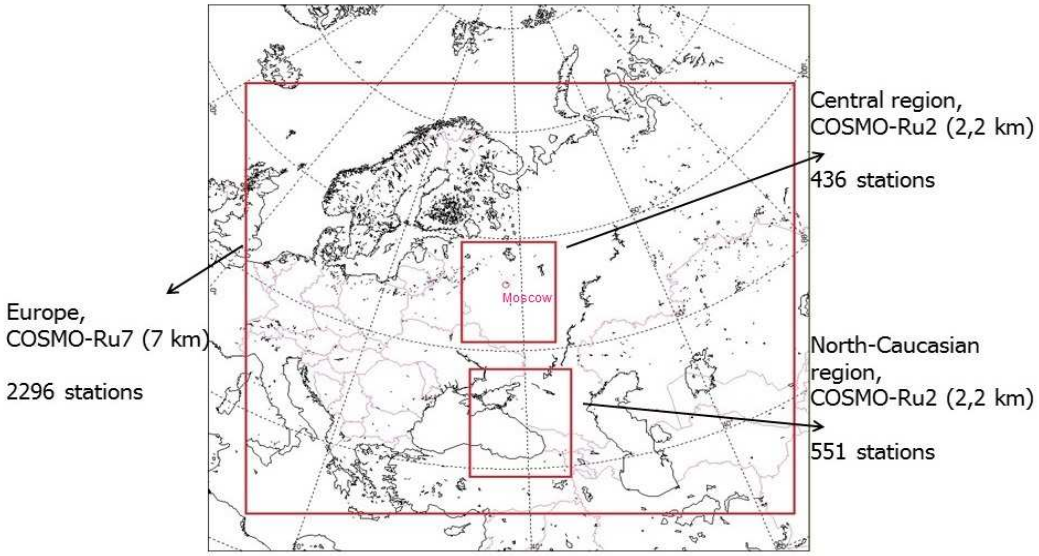

Figure 3: Regions of COSMO-Ru.

5 Verification of COSMO-Ru forecasts calculated operationally and according to SNOWE technology

Verification of results of the proposed technology was done in VERSUS mostly for spring period of snow melting period during 2014/2015 snow season.

Small improvement of RMSE of T2m COSMO-Ru7 forecasts in case of using the proposed technology can be observed (graphs were produced for approximately 800 stations). Such a result points to the fact that conditional verifications needed to reveal the expected effect, as the territory of COSMO-Ru7 region is large and snow boundary migrates daily.

An example of efficiency of new technology is shown on Fig.5. ME and RMSE values for air temperature for COSMO-Ru7 area were reduced (RMSE for 0,5-1,5^{o}C and ME for 0,5-1,0^{o}C), especially for the 3d day of the forecast (Fig.5-6). Errors in positive T2m forecasts are greater than in negative. Improvement in T2m forecasts using proposed technology is observed both for positive and negative T2m.

For Central Russia (COSMO-Ru2 model) such dependence can be recorded only through separate dates (Fig.7, Table 1) since the territory (area of integration) is not big enough to 'catch' moving of snow boundary during snow melting period.

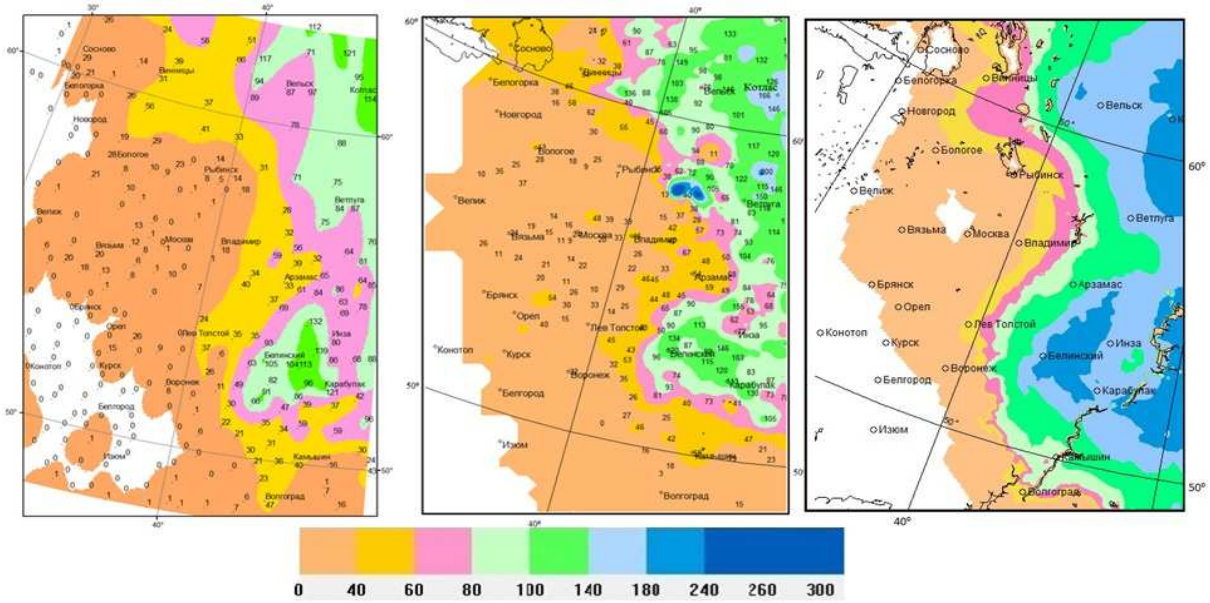

Figure 4: Maps of SWE (mm) obtained on the basis of SMFE calculations (left), with the help of graphical package 'GIS Meteo' by snow surveys' data (center) and SWE initial fields for COSMO-Ru7 (right). 28 Feb 2014.

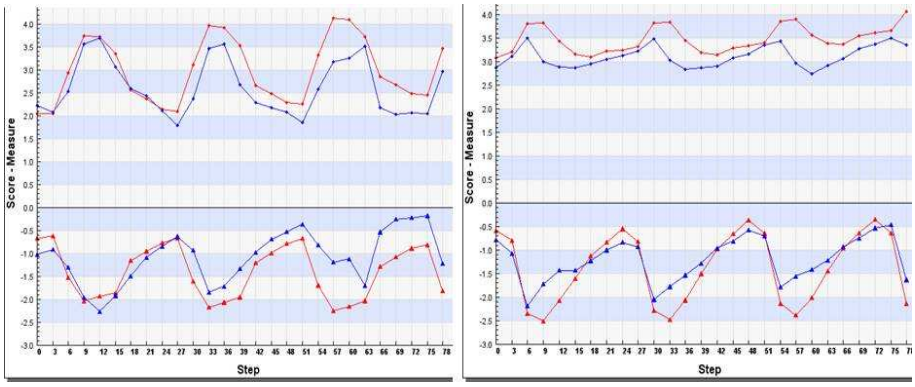

Figure 5: ME (bottom lines) and RMSE (upper lines) values for air temperature(^{o}) forecasts for the COSMO-Ru7 area according to operational (red dots) and experimental (blue dots) modes for 24 Feb-31 March 2015. Left- when positive air temperatures were observed at the stations, right-upon condition when negative.

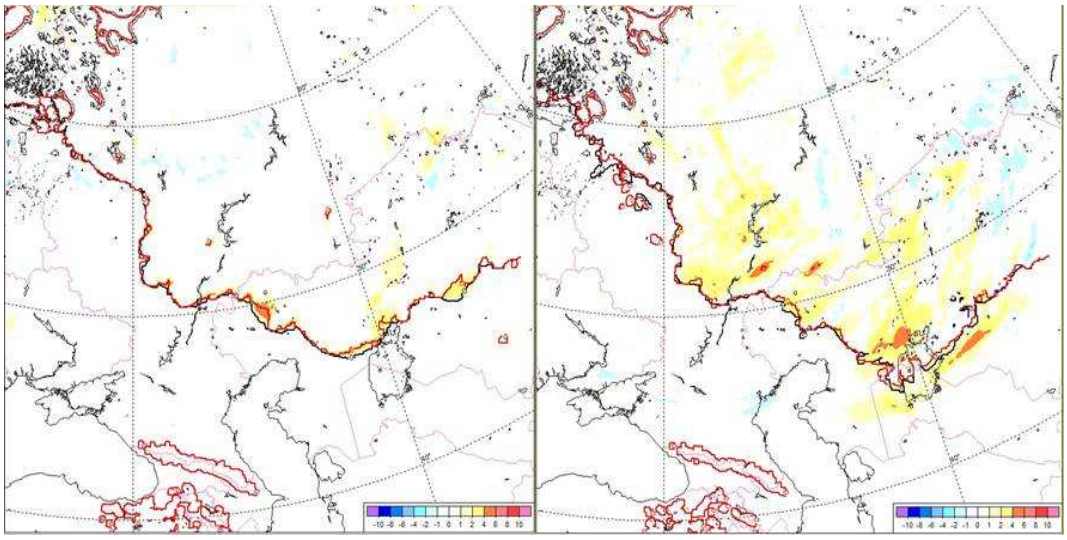

Figure 6: Difference between air temperature (^oC) forecasts at 12 UTC (left) and 78 UTC (right) for the COSMO-Ru7 area according to operational and experimental modes. 25 March 2015.

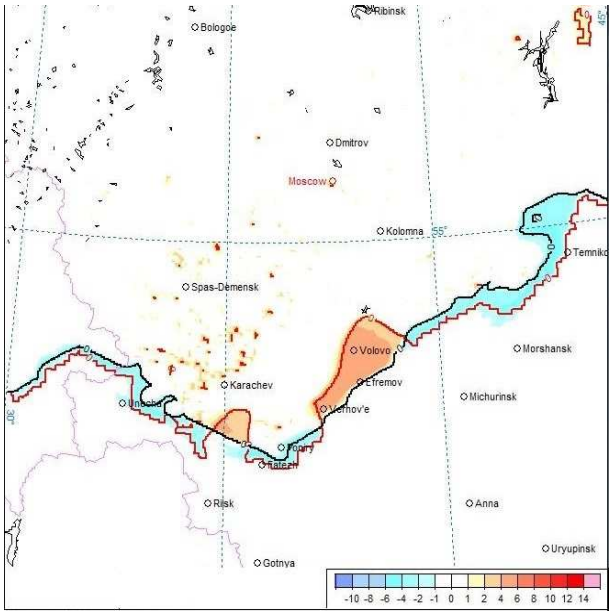

Figure 7: Difference between air temperature (^oC) forecasts at 12 UTC for the COSMO-Ru2 area (Central Russia) according to operational and experimental modes. 10 April 2013.

Table 1: T2m (^{o}) for 12 UTC and 00 UTC at stations situated close to the snow boundary according to observations and forecasts for 12 and 24 hours for operational and experimental modes of COSMO-Ru2 technology

	10 April 2013, 12 UTC			11 April 2013, 00 UTC		
Station	Obs t^oC	Operational mode t^oC / abs. error,°C accuracy%	Experiment t^oC /abs. error,°C accuracy%	Obs t^oC	Operational mode t^oC / abs. error,°C accuracy%	Experiment t^oC / abs. error,°C accuracy%
Efremov	8.1	4.3/ 3.7/0	6.6 /1.4/ 100	-0.4	-0.5/ 0.1/ 100	-0.6/ 0.2/ 100
Volovo	6.9	0.6/ 6.3/ 0	5.8 /1.1/ 100	-1.1	-3.6/ 2.5/ 100	-1.7/ 0.6/ 100
Verhov'e	7.0	1.2/ 5.8/ 0	6.0 /1.0/ 100	0.8	-1.2/ 2.0/ 100	-0.2/ 1.0/ 100
Temnikov	7.2	6.2/ 1.0/ 100	5.6 /1.6/ 100	0.2	0.7/ 0.5/ 100	-3.0/ 2.8/ 100
Unecha	7.1	6.6/ 0.5/100	5.4 /1.7/ 100	1.0	0.4/ 0.6/ 100	0.7/ 0.3/ 100
Fatezh	8.1	5.6/ 2.5/100	6.7 /1.4/ 100	-1.5	-3.0/ 1.5/ 100	0.3/ 1.8/ 100
Mean abs. error, °C / mean accuracy,%		3.3°C /50%	1.4°C /100%		1.2°C / 100%	1.1°C / 100%

Comparing T2m forecasts for the case with significant cloudiness- total cloud cover($TCC \geq 75\%$, overcast) with the case of insignificant prognostic cloudiness ($TCC \leq 25\%$, clear sky) the proposed technology provides some differences in their prognostic values for the first day of the forecast shown at Fig.8.

It can be related to the local TCC changes in the COSMO-model. If we take into account both prognostic and observed values of TCC Fig.9), significant improvements of RMSE and ME are observed for clear sky both for positive and negative values of observed T2m (Fig.9-11). For forecasts when $TCC \geq 75\%$ improvement of RMSE for positive temperatures occurs for 2-3 forecast days, for negative - it is not so pronounced (RMSE decreases, ME increases). Proposed technology improves T2m forecasts for cases of mostly positive T2m at clear sky conditions.

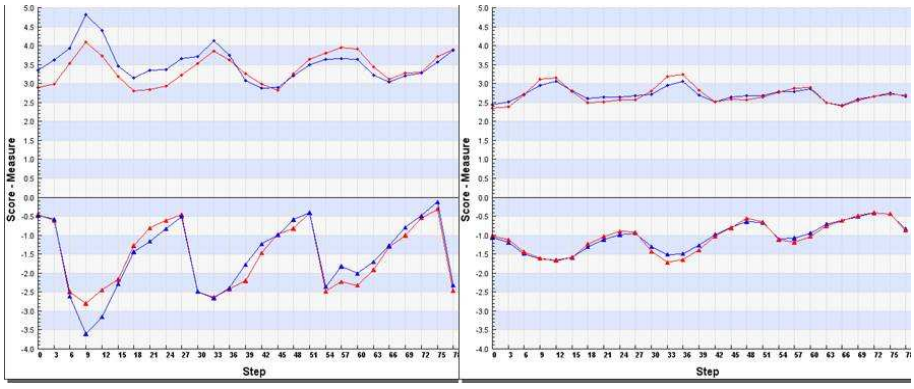

Figure 8: ME (bottom lines) and RMSE (upper lines) values for air temperature (^{o}C) forecasts for the COSMO-Ru7 area according to operational (red dots) and experimental (blue dots) modes for 24 Feb-31 March 2015. Left-upon condition that prognostic $TCC \leq 25\%$, right-upon condition it was $\geq 75\%$.

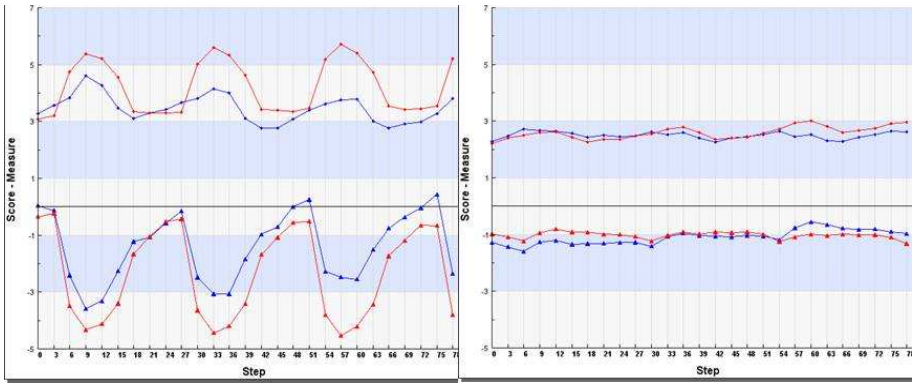

Figure 9: ME (bottom lines) and RMSE (upper lines) values for air temperature (^{o}C) forecasts for the COSMO-Ru7 area according to operational (red dots) and experimental (blue dots) modes for 24 Feb-31 March 2015. Left-upon condition that both prognostic and observed TCC was $\leq 25\%$, right-upon condition that it was$\geq 75\%$.

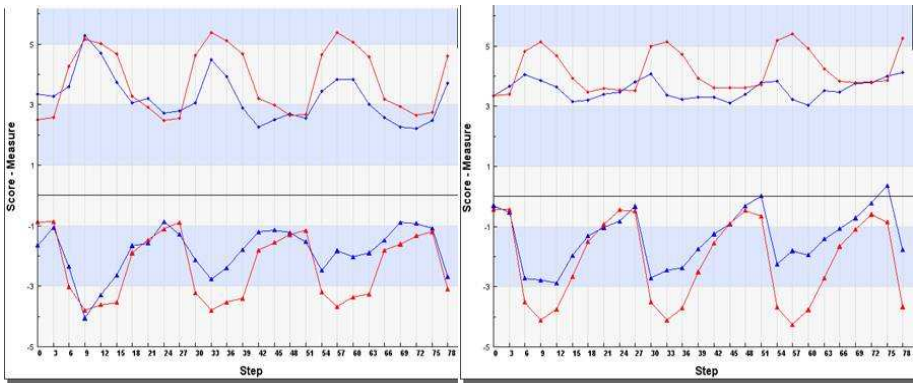

Figure 10: ME (bottom lines) and RMSE (upper lines) values for air temperature (^{o}C) forecasts for the COSMO-Ru7 area according to operational (red dots) and experimental (blue dots) modes for 24 Feb-31 March 2015. Left-upon conditions that prognostic TCC was $\leq 25\%$ and positive air temperatures were observed at stations, right-upon condition that TCC was $\geq 75\%$ and negative air temperatures were observed at stations.

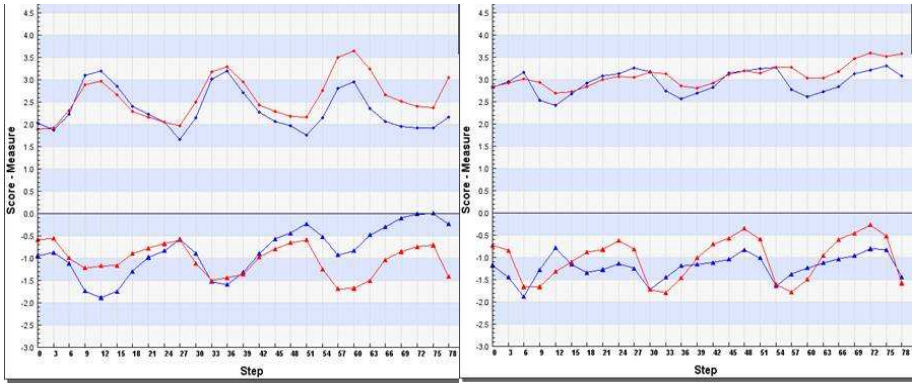

Figure 11: ME (bottom lines) and RMSE (upper lines) values for air temperature (°C) forecasts for the COSMO-Ru7 area according to operational (red dots) and experimental (blue dots) modes for 24 Feb-31 March 2015. Left-upon conditions that prognostic TCC was $\geq 75\%$ and positive air temperatures were observed at stations, right-upon condition that TCC was $\geq 75\%$ and negative air temperatures were observed at stations.

Changes in improvement T2m forecasts are observed both for COSMO-Ru2 and COSMO-Ru7 technologies when snow is present (Fig.12). The thinner snow cover is (case of snow depth ≤ 5 cm), the more probability we have that it will melt during the forecast time (see decreasing of RMSE and ME in time scale in Fig.12).

Consequently, the main conclusion follows from verification of T2m COSMO-model forecasts using the proposed technology with modified initial SWE and snow density fields, is that the largest improvement of T2m forecasts is in case of positive temperatures under clear sky conditions, and thin snow cover, i.e. in the areas close to snow boundary.

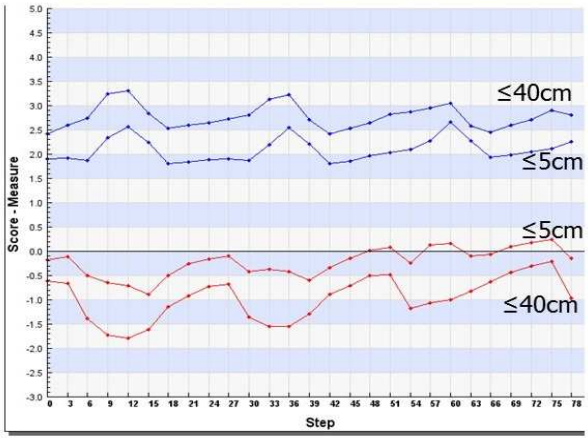

Figure 12: ME (red lines) and RMSE (blue lines) values for air temperature (°C) forecasts for the COSMO-Ru7 area according to experimental mode upon conditions that prognostic snow depth ≤ 5 cm and ≤ 40 cm for 24 Feb-31 March 2015.

Differences between two technologies in TCC forecasts are mostly observed on cloud edges and in the zones of rare cloudiness (Fig.13).

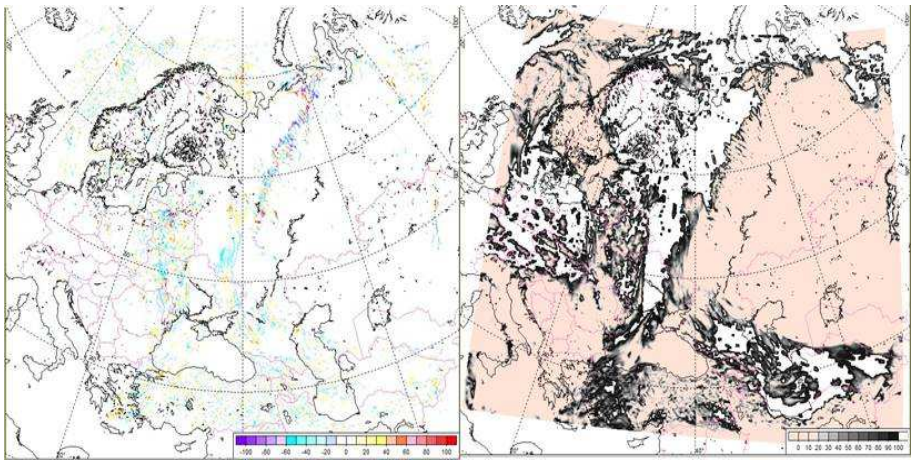

Figure 13: TCC (%) forecast at 12 UTC for the COSMO-Ru7 area according to experimental mode of COSMO-Ru7 (right) and its difference with operational mode (left). 31 March 2015.

When modifying initial fields of SWE and snow density, prognostic values of these snow characteristics will also be changed (Fig.14). Differences in albedo between two technologies will be observed in area close to the snow boundary (Fig.15). Albedo and TCC modifications will affect the radiative balance and, hence changes in heat fluxes occure (see example in Fig.16).

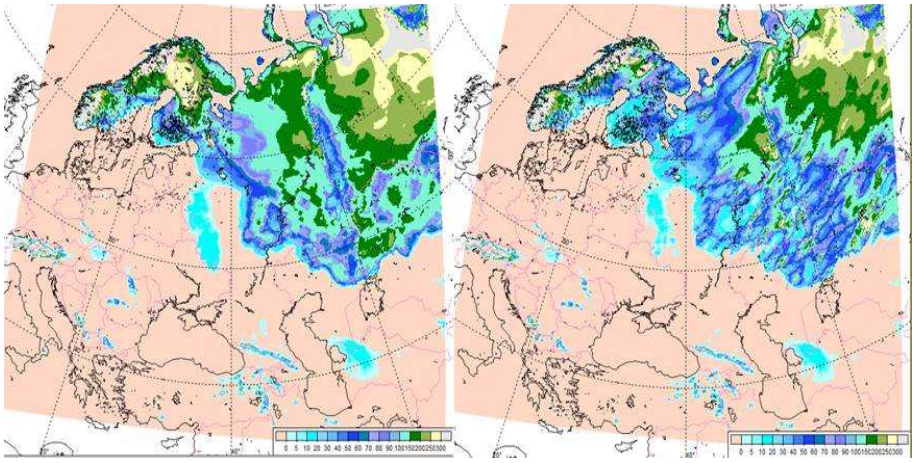

Figure 14: SWE (mm) forecasts at 12 UTC for the COSMO-Ru7 area according to operational (left) and experimental (right) modes of COSMO-Ru7. 31 March 2015.

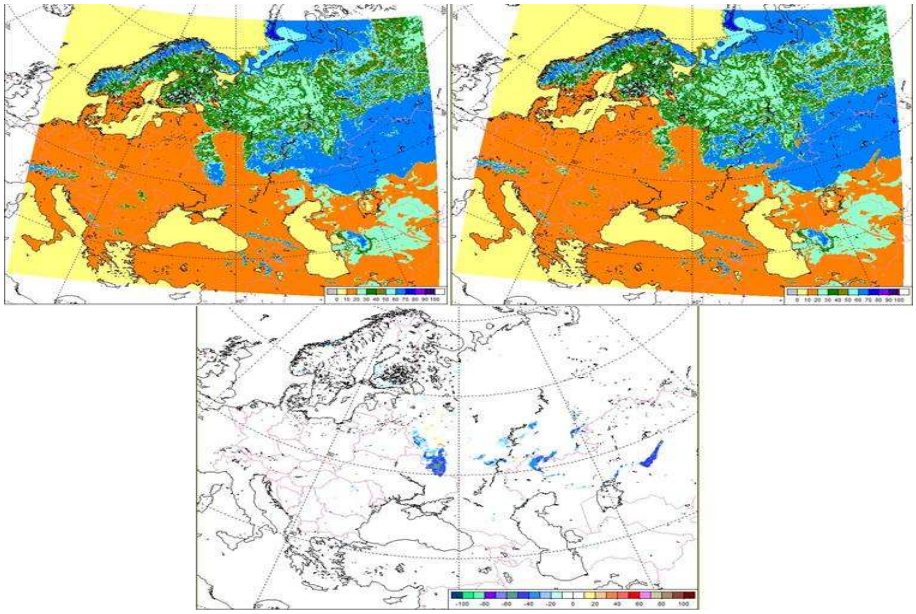

Figure 15: Albedo (%) forecasts at 12 UTC for the COSMO-Ru7 area according to operational (left) and experimental (right) modes of COSMO-Ru7. Bottom-difference between experimental and operational modes. 31 March 2015.

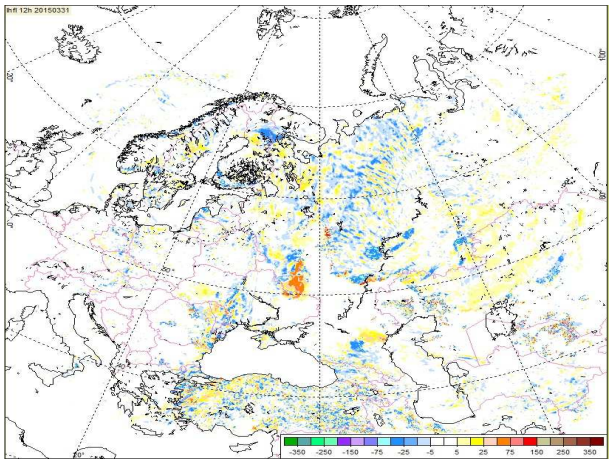

Figure 16: Difference between latent heat flux (W/m^2) forecasts at 12 UTC for the COSMO-Ru7 area according to operational and experimental modes of COSMO-Ru7. 31 March 2015.

Changes in 10 m wind speed forecasts using the proposed technology can be detected only locally, the graphs for errors between two technologies don't give specific differences (Fig.17). Assessment of ME and RMSE for 10m wind speed in positive air temperature range observed at stations doesn't show clear advantage of proposed technology. RMSE decrease at 18-24 UTC (especially for the 3d day of the forecast) while ME increase.

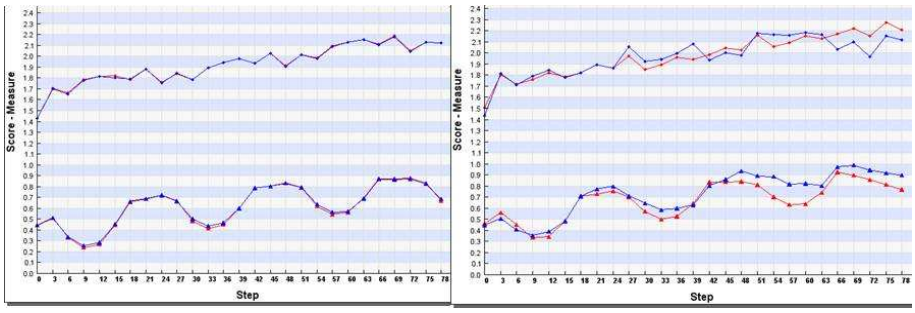

Figure 17: ME (bottom lines) and RMSE (upper lines) values for 10m wind speed (m/s) forecasts for the COSMO-Ru7 area according to operational (red dots) and experimental (blue dots) modes for 24 Feb-10 April 2015. Right-upon condition that positive air temperatures were observed at stations, left-without conditions.

Thus, local changes in forecasts of 10 m wind speed and cloudiness were also found, however distribution of special patterns of their occurrence were not indicatively diagnosed. It is demonstrated that modifications in initial fields of SWE and snow density are consistent with the standard COSMO forecast and lead to improvements of surface variables' forecast (especially T2m).

Conclusions

The SNOWE technology was realized in operational technologies COSMO-Ru for the winter of 2014/2015. The implementation of SNOWE technology showed the positive impact for SWE forecasts as well as for T2m forecasts near the snow boundary. The more realistic forecast of SWE based on the SNOWE corrected initial data provides more realistic speed of movements of snow boundary during the forecast time.

The largest improvement (2-3^{o}C after averaging and up to 7^{o}C for particular cases) is observed for T2m forecasts in the cases of clear sky conditions and cases with thin snow cover. Some influence is indicated for total cloud cover, 10m wind speed forecasts as well as for heat fluxes and surface albedo.

References

[1] Bartlett P.A, MacKay M.D., Verseghy D.L., 2006. Modified Snow Algorithms in the Canadian Land Surface Scheme: Model Runs and Sensitivity Analysis at Three Boreal Forest Stands. Atmosphere-Ocean, Canadian Meteorological and Oceanographic Society, 43 (3), **207-222**.

[2] Epifanov V., Osokin N., 2010. Research of strength properties of snow on a mountain slope of the Spitsbergen archipelago. Earth's cryosphere, vol. XIV, No.1, **81-91** (in Russian).

[3] Kazakova E., Chumakov M., Rozinkina I., 2013. Realization of the parametric snow cover model SMFE for snow characteristics calculation according to standard net meteorological observations. COSMO Newsletter, No.13, **39-49**.

[4] Kazakova E., Rozinkina I., 2011. Testing of Snow Parameterization Schemes in COSMO-Ru: Analysis and Results. COSMO Newsletter, No.11,**41-51**.

[5] Kuzmin P. Process of Snow Cover Melting. Leningrad, Hydrometeoizdat, 1961, **345** (in Russian).

[6] Yosida Z., Huzioka T., 1954. Some Studies of the Mechanical Properties of Snow. IAHS Red Book Series. Publ. no. 39, Gentbrugge, **98-105**.